

See discussions, stats, and author profiles for this publication at: <https://www.researchgate.net/publication/231700227>

# Impact of Surface-Modified Nanoparticles on Glass Transition Temperature and Elastic Modulus of Polymer Thin Films

ARTICLE *in* MACROMOLECULES · OCTOBER 2007

Impact Factor: 5.8 · DOI: 10.1021/ma071332s

---

CITATIONS

27

---

READS

119

6 AUTHORS, INCLUDING:



Edwin P Chan

National Institute of Standards and Technolo...

39 PUBLICATIONS 1,037 CITATIONS

SEE PROFILE

# Impact of Surface-Modified Nanoparticles on Glass Transition Temperature and Elastic Modulus of Polymer Thin Films

Jong-Young Lee,<sup>†</sup> Kristin E. Su,<sup>‡</sup> Edwin P. Chan,<sup>†</sup> Qingling Zhang,<sup>†</sup> Todd Emrick,<sup>†</sup> and Alfred J. Crosby\*,<sup>†</sup>

Department of Polymer Science and Engineering, University of Massachusetts, Amherst, Massachusetts 01003, and Department of Chemistry, University of Massachusetts, Amherst, Massachusetts 01003

Received June 15, 2007

Revised Manuscript Received September 10, 2007

To take advantage of unique and enhanced properties for nanoparticle-filled materials, the nanoparticles must be well-dispersed.<sup>1,2</sup> Surface modification of the particles with matrix-compatible ligands is one of the most effective strategies to improve polymer–nanoparticle compatibility and ensure dispersion.<sup>3–5</sup> Because of the large surface area per volume of the nanoparticle, the ligands play a significant role in determining the properties of the nanoparticle. Although the role of the ligand is more defined when it establishes high strength bonds with the surrounding matrix,<sup>6–10</sup> its role in material properties is less clear when enthalpic interactions are neglected, leaving entropy as a significant factor.<sup>9,10</sup> To provide insight into the physical mechanisms that control material properties in polymer nanocomposites, we have designed a model material system to simultaneously disperse nanoparticles and emphasize entropic effects. Here, we report the impact of this design on the elastic modulus and glass transition temperature ( $T_g$ ) of the polymer nanocomposites. We focus on the impact of nanoparticle weight fraction and develop relationships to decouple the roles of inorganic particles and ligand molecules in defining nanocomposite properties.

A nanocomposite of cadmium selenide (CdSe) nanoparticles, 3.5 nm in diameter, blended into a polystyrene (PS) matrix (MW = 131K g/mol, PDI = 1.02, Polymer Source Inc.) served as the model material. To attain well-dispersed nanoparticles within the polystyrene matrix, short polystyrene ligands (MW = 1000 g/mol) were used to functionalize the nanoparticle surfaces. In addition to aiding nanoparticle dispersion, the enthalpic interaction and entanglement between nanoparticles and polymer matrix are minimized due to the surface-grafted PS chains. Detailed information about the PS–CdSe nanoparticle synthesis and dispersion within a PS matrix is given in previous publications.<sup>11,12</sup> Solutions of nanoparticles and PS in toluene were prepared, with varying nanoparticle weight percentage, to facilitate the casting of nanocomposite films.

To measure the elastic modulus of the nanocomposite thin films, we used SIEBIMM (strain-induced elastic buckling instability for mechanical measurements).<sup>13</sup> In short, this technique involves floating a thin polymer film onto a thick, cross-linked polydimethylsiloxane (PDMS) substrate (Dow Corning Sylgard 184, weight ratio of prepolymer to cross-linker is 1:20; cured at 70 °C for 2 h). After drying the film/PDMS bilayer for 24 h, the bilayer is strained uniaxially in a custom-built, automated strain stage. Because of the large difference in

modulus between the nanocomposite film and PDMS substrate, a net compressive stress develops orthogonal to the tensile direction and buckles the nanocomposite thin film. By measuring the buckling wavelength ( $\lambda$ ), the modulus of the polymer film ( $E_p$ ) can be obtained:

$$E_p = \frac{1 - \nu_p^2}{1 - \nu_{PDMS}^2} 3E_{PDMS} \left( \frac{\lambda}{2\pi h} \right)^3$$

$E_{PDMS}$  is the elastic modulus of the PDMS substrate, as measured using a contact mechanical test.<sup>14</sup> We assume the Poisson's ratio of the PDMS substrate and polymer film are  $\nu_{PDMS} = 0.5$  and  $\nu_p = 0.33$ , respectively. The thickness of the nanocomposite thin films,  $h$ , is controlled by flow coating and quantified by interferometry (Filmetrics Inc.).<sup>15</sup> The film thickness used in the experiments ranged from 180 to 210 nm.  $\lambda$  is the periodic wavelength of buckles obtained by fast Fourier transform (FFT) of optical images.

The  $T_g$  of these thin films is measured by differential scanning calorimetry (DSC). For the DSC measurement, the nanocomposite film was floated on water and transferred to a DSC sample holder. The samples were dried under vacuum at room temperature for 24 h before performing the  $T_g$  measurement. Nanoparticles may reorganize due to entropy-driven mobility during heating;<sup>16–21</sup> therefore, the  $T_g$  of the nanocomposite is determined from the first heating cycle for all samples (heating rate is 10 °C/min). All samples are prepared by solution casting and dried at room temperature to maintain the same thermal history. Therefore,  $T_g$  obtained from first-run heating were not affected by the difference in thermal history among samples. Representative data from DSC and SIEBIMM measurements are provided in the Supporting Information.

In general, adding rigid particles into a polymer matrix increases the elastic modulus of the material as a function of volume or weight fraction of particles.<sup>8,22</sup> However, the elastic modulus of the nanocomposite films studied here was found to decrease as a function of nanoparticle weight fraction ( $W$ ) (Figure 1). In a consistent manner, the  $T_g$  decreased as a function of  $W$  (Figure 1). These effects can be attributed to two mechanisms. One is a plasticizing effect of the surface-bound PS ligands, in which the low molecular weight of the ligands (MW = 1000 g/mol) provides an expected decrease in both  $T_g$  and modulus.<sup>23</sup> The second mechanism is linked to the configuration of polymer chains near nanoparticles with minimal enthalpic interactions with the matrix. According to simulation results,<sup>24,25</sup> when the enthalpic interaction between the particles and surrounding matrix is weak or neutral, a reduction in monomer density at a rigid particle–matrix interface occurs due to entropically driven repulsion of the polymer chains from the nanoparticle surface. A schematic plot of “monomer vs distance” is shown in Figure 2. This decreased density leads to the increase in chain mobility and consequently a depression in  $T_g$ .<sup>25</sup> This mechanism is consistent with reports of  $T_g$  depression in experiments with poorly bound (or nonwetting) interfaces between the particles and polymer matrix.<sup>9,10,26,27</sup>

To decouple these two possible mechanisms, we compare the material properties of the nanocomposite PS system to a simple blend of short PS chains and a PS matrix. The polymer blend consists of low molecular weight PS (MW = 1000 g/mol, the same molecular weight of the nanoparticle-bound ligands) as a “plasticizer” in a PS matrix (MW = 131K g/mol, the same

\* To whom correspondence should be addressed: e-mail crosby@mail.pse.umass.edu; Tel (413) 577-1313; Fax (413) 542-0082.

<sup>†</sup> Department of Polymer Science and Engineering.

<sup>‡</sup> Department of Chemistry.

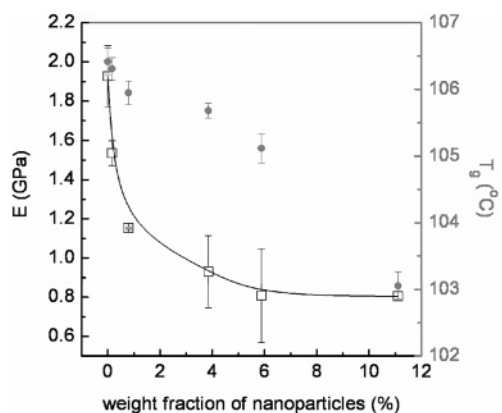


**Figure 1.** Plot of elastic modulus ( $E$ , hollow squares) and  $T_g$  (solid circles) as a function of weight fraction of nanoparticles.

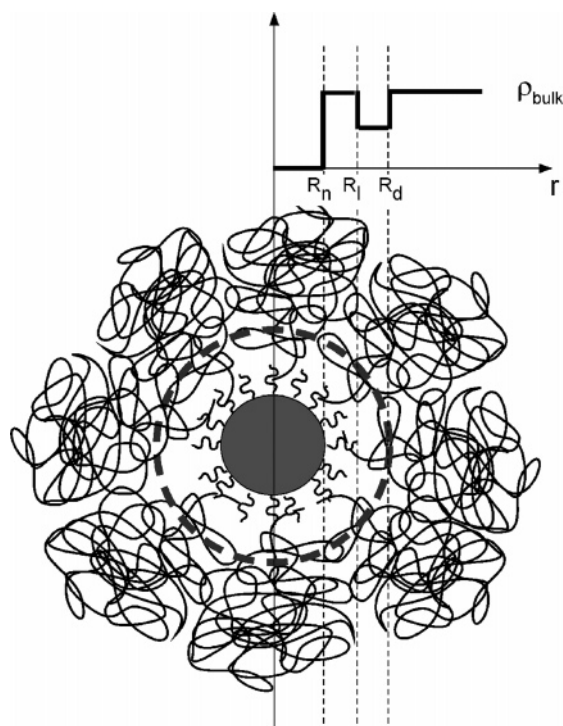


**Figure 2.** Top: schematic plot of “monomer density ( $\rho$ ) vs distance ( $r$ )”.  $R_n$  is the radius of a nanoparticle.  $R_l$  is the distance from the center of a nanoparticle to the end of ligands.  $R_d$  is the distance from the center of a nanoparticle to the interface of low-density area region and bulk PS. Bottom: schematic morphology of polymer chains around a nanoparticle with neutral enthalpic interaction.

molecular weight used as the matrix in the polymer nanocomposites). To facilitate comparison and isolate the effect of the surface ligands, we quantify the weight fraction of the surface ligands in the nanoparticle–polymer composite. On the basis of thermogravimetric analysis (TGA), we determine the weight fraction of surface ligands to nanoparticle  $\sim 4\%$ . Consequently, the weight fraction of surface ligands relative to matrix polymer chains can be determined for different filler/matrix weight fractions.

On the basis of the Flory–Fox equation<sup>28</sup> and the assumption that the  $T_g$  for the PS matrix (MW = 130K g/mol) is close to the  $T_g$  for an infinitely long PS molecule,  $T_g$  depression ( $\Delta T_g$ ) for a miscible blend is

$$\Delta T_g = T_g - T_{g,\infty} = (T_{g,1} - T_{g,\infty})W$$

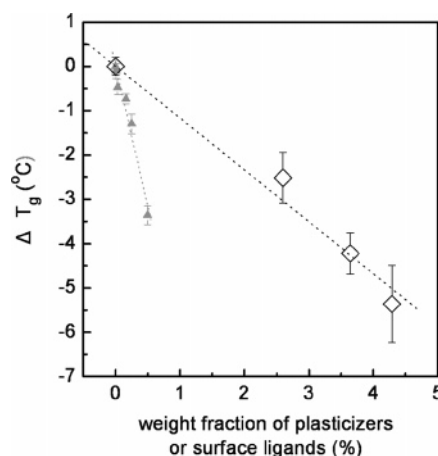


**Figure 3.** Plot of  $\Delta T_g$  as a function of weight fraction of the plasticizer (PS, MW = 1000) in the polymer blend (hollow diamonds) and surface ligands in polymer nanocomposites (solid triangles).

$T_g$  and  $T_{g,\infty}$  are the glass transition temperature of the polymer blend and homopolymer with infinite molecular weight, respectively.  $W$  is the weight fraction of the blended component. For both the polymer blend and nanocomposite systems, a linear relationship between  $\Delta T_g$  and weight fraction of ligands/plasticizers is observed (Figure 3). From measured values of  $T_g$  for the PS matrix ( $T_{g,\infty} = 107^\circ\text{C}$ ) and best-fit linear slopes in Figure 3,  $T_{g,1}$  of the plasticizers and surface ligands can be obtained. We determine  $T_{g,1} = 2^\circ\text{C}$  for the plasticizer and  $-526^\circ\text{C}$  for the nanoparticle-bound surface ligands. The  $T_g$  for the plasticizer is comparable to independent DSC measurements on 100% PS (MW = 1000 g/mol)  $\sim 7^\circ\text{C}$ , but the value for the surface-bound ligands is clearly unrealistic. DSC measurements on a sample of pure nanoparticles (weight fraction is 100%) gave a  $T_g$  of  $0^\circ\text{C}$ . Therefore, this result implies that another mechanism is contributing to the lower  $T_g$  of the nanocomposites.

As mentioned previously, when enthalpic interactions are neglected, monomer density near the nanoparticle surface is lower than the bulk due to entropic effects (Figure 2). Therefore, polymer segments in this low-density region have higher mobility and associated lower  $T_g$ . Accounting for these additional polymer segments with a lower  $T_g$  would effectively increase the weight fraction of “surface ligands” for the nanocomposite data in Figure 3.

In Figure 3, the slope of the surface ligands is 6 times that of the plasticizers, thus implying that the polymer chains in the low density area ( $R_l < r < R_d$  in Figure 2) give an additional 5 times weight fraction of low molecular weight polymer in the matrix. Assuming the density of polymer segments in the low-density region ( $R_l < r < R_d$  in Figure 2) equals the density of surface ligands ( $R_n < r < R_l$  in Figure 2), we can use the difference in the slopes ( $K$ ) to estimate  $R_d$  on the basis of volume arguments:

$$\frac{R_d}{R_n} = \left[ K \left( \left( \frac{R_l}{R_n} \right)^3 - 1 \right) + 1 \right]^{1/3}$$

$R_n$  (Figure 2) is the radius of a nanoparticle, equal to 1.75 nm in our materials.  $R_l$  is the distance from the center of a nanoparticle to the end of ligands, which is 2.75 nm if the fully extended conformation of ligands is assumed (ligand length is  $\sim 1$  nm).  $R_d$  is the distance from the center of a nanoparticle to the interface of low density area region and bulk PS, which is

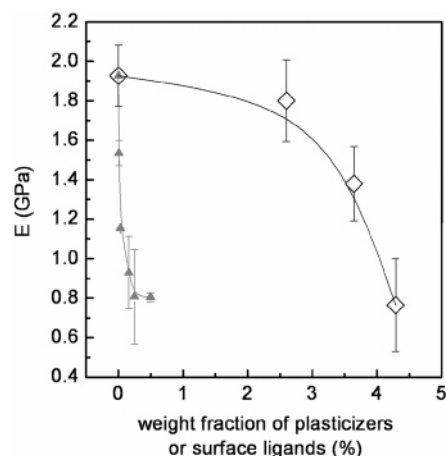


**Figure 4.** Plot of elastic modulus ( $E$ ) as a function of weight fraction of the plasticizer (PS, MW = 1000) in the polymer blend (hollow diamonds) and surface ligands in polymer nanocomposites (solid triangles).

~4.6 nm based on a measured value of  $K = 6$ . Consequently, the affected range of neighboring polymer segments is 1.85 nm ( $R_d - R_l$ ), close to the length scale described in molecular dynamics simulation<sup>25</sup> and in accord with our hypothesis that the entropic contributions are a plausible mechanism for the decrease in  $T_g$  exhibited by the nanocomposite samples. Although this estimate is based on local changes, we have not accounted for self-concentration effects or the effects of spatial heterogeneities within the PS matrix,<sup>29,30</sup> which may be on similar length scales to our nanoparticles. Our materials may provide an interesting system for considering these contributions in future experiments.

Similar to our measurements for  $T_g$ , the elastic moduli for the blend of PS (MW = 131K g/mol) and PS (MW = 1000 g/mol) are compared to the nanocomposite as a function of weight fraction of surface ligands and plasticizers (Figure 4). In the nanocomposite system, the elastic modulus decreases significantly at low weight fraction of surface ligands. However, this trend is not observed for the polymer blend system. The trend of modulus decreasing as a function of weight fraction for the polymer blend system is similar to the results reported previously.<sup>13,23</sup> Therefore, similar to the  $T_g$  effect, we attribute the trend exhibited by the nanocomposite to the decreased polymer segment density near the rigid filler surface. More details for this mechanism will be explored in future investigations.

In conclusion, we have demonstrated that the addition of rigid nanoparticles with minimal enthalpic interactions with a surrounding polymer matrix leads to a decrease in the elastic modulus and  $T_g$ . The properties of surface ligands attached to the nanofillers must be properly considered for the design of nanocomposite systems. The effect of the nanoparticles on the conformation of neighboring polymer chains leads to depressed  $T_g$  and elastic modulus values. The rate of  $T_g$  and elastic modulus depression as a function of weight fraction of nanoparticles is determined by (1) the properties of the surface ligands, (2) the

strength of particle–matrix enthalpic interaction, and (3) the entropy-driven surface effects which are related to the relative length scale between particles, surface ligands, and matrix chains.

**Acknowledgment.** Funding for this project is provided by the NSF-MRSEC at the University of Massachusetts, Petroleum Research Fund of the American Chemical Society, and the Department of Energy (DE-FG-02-96ER45).

**Supporting Information Available:** Representative data from DSC and SIEBIMM measurements. This material is available free of charge via the Internet at <http://pubs.acs.org>.

## References and Notes

- (1) Jordan, J.; Jacob, K. I.; Tannenbaum, R.; Sharaf, M. A.; Jasiuk, I. *Mater. Sci. Eng., A* **2005**, *393*, 1–11.
- (2) Thostenson, E. T.; Li, C. Y.; Chou, T. W. *Compos. Sci. Technol.* **2005**, *65*, 491–516.
- (3) Bontempo, D.; Tirelli, N.; Feldman, K.; Masci, G.; Crescenzi, V.; Hubbell, J. A. *Adv. Mater.* **2002**, *14*, 1239–1243.
- (4) Skaff, H.; Emrick, T. *Angew. Chem., Int. Ed.* **2004**, *43*, 5383–5386.
- (5) Sill, K.; Emrick, T. *Chem. Mater.* **2004**, *16*, 1240–1243.
- (6) Vollenberg, P. H. T.; Heikens, D. *Polymer* **1989**, *30*, 1656–1662.
- (7) Vollenberg, P. H. T.; Dehaan, J. W.; Vandeven, L. J. M.; Heikens, D. *Polymer* **1989**, *30*, 1663–1668.
- (8) Ji, X. L.; Jing, J. K.; Jiang, W.; Jiang, B. Z. *Polym. Eng. Sci.* **2002**, *42*, 983–993.
- (9) Bansal, A.; Yang, H. C.; Li, C. Z.; Benicewicz, R. C.; Kumar, S. K.; Schadler, L. S. *J. Polym. Sci., Part B: Polym. Phys.* **2006**, *44*, 2944–2950.
- (10) Rittigstein, P.; Torkelson, J. M. *J. Polym. Sci., Part B: Polym. Phys.* **2006**, *44*, 2935–2943.
- (11) Peng, Z. A.; Peng, X. G. *J. Am. Chem. Soc.* **2001**, *123*, 183–184.
- (12) Lee, J.-Y.; Zhang, Q.; Emrick, T.; Crosby, A. J. *Macromolecules* **2006**, *39*, 7392.
- (13) Stafford, C. M.; Harrison, C.; Beers, K. L.; Karim, A.; Amis, E. J.; Vanlandingham, M. R.; Kim, H. C.; Volksen, W.; Miller, R. D.; Simonyi, E. E. *Nat. Mater.* **2004**, *3*, 545–550.
- (14) Shull, K. R.; Ahn, D.; Chen, W. L.; Flanagan, C. M.; Crosby, A. J. *Macromol. Chem. Phys.* **1998**, *199*, 489–511.
- (15) Lee, J.-Y.; Crosby, A. J. *Macromolecules* **2005**, *38*, 9711–9717.
- (16) Bockstaller, M. R.; Lapetnikov, Y.; Margel, S.; Thomas, E. L. *J. Am. Chem. Soc.* **2003**, *125*, 5276–5277.
- (17) Gupta, S.; Zhang, Q. L.; Emrick, T.; Balazs, A. C.; Russell, T. P. *Nat. Mater.* **2006**, *5*, 229–233.
- (18) Lee, J. Y.; Buxton, G. A.; Balazs, A. C. *J. Chem. Phys.* **2004**, *121*, 5531–5540.
- (19) Lee, J. Y.; Thompson, R. B.; Jasnow, D.; Balazs, A. C. *Phys. Rev. Lett.* **2002**, *89*.
- (20) Thompson, R. B.; Ginzburg, V. V.; Matsen, M. W.; Balazs, A. C. *Science* **2001**, *292*, 2469–2472.
- (21) Tyagi, S.; Lee, J. Y.; Buxton, G. A.; Balazs, A. C. *Macromolecules* **2004**, *37*, 9160–9168.
- (22) Ahmed, S.; Jones, F. R. *J. Mater. Sci.* **1990**, *25*, 4933–4942.
- (23) Sears, J. K.; Darby, J. R. *The Technology of Plasticizers*; Wiley: New York, 1982.
- (24) Ozmusul, M. S.; Picu, R. C. *Polymer* **2002**, *43*, 4657–4665.
- (25) Starr, F. W.; Schroder, T. B.; Glotzer, S. C. *Macromolecules* **2002**, *35*, 4481–4492.
- (26) Ash, B. J.; Siegel, R. W.; Schadler, L. S. *J. Polym. Sci., Part B: Polym. Phys.* **2004**, *42*, 4371–4383.
- (27) Bansal, A.; Yang, H. C.; Li, C. Z.; Cho, K. W.; Benicewicz, B. C.; Kumar, S. K.; Schadler, L. S. *Nat. Mater.* **2005**, *4*, 693–698.
- (28) Fox, T. G.; Flory, P. J. *J. Appl. Phys.* **1950**, *21*, 581–591.
- (29) Ediger, M. D. *Annu. Rev. Phys. Chem.* **2000**, *51*, 99–128.
- (30) Lutz, T. R.; He, Y. Y.; Ediger, M. D. *Macromolecules* **2005**, *38*, 9826–9835.

MA071332S